Iowa State University

From the SelectedWorks of Martin M. Thuo

November, 2013

Defining the Value of Injection Current and Effective Electrical Contact Area for EGaIn-Based Molecular Tunneling Junctions

Felice C. Simeone, *Harvard University*
Hyo Jae Yoon, *Harvard University*
Martin M. Thuo, *Harvard University*
Jabulani R. Barber, *Harvard University*
Barbara Smith, *Harvard University*, et al.

Available at: http://works.bepress.com/martin_thuo/9/

SelectedWorks™

J|A|C|S
JOURNAL OF THE AMERICAN CHEMICAL SOCIETY
Article
pubs.acs.org/JACS

Defining the Value of Injection Current and Effective Electrical Contact Area for EGaIn-Based Molecular Tunneling Junctions

Felice C. Simeone, Hyo Jae Yoon, Martin M. Thuo, Jabulani R. Barber, Barbara Smith, and George M. Whitesides*

Department of Chemistry and Chemical Biology, Harvard University, Cambridge, Massachusetts 02138, United States

Ⓢ *Supporting Information*

ABSTRACT: Analysis of rates of tunneling across self-assembled monolayers (SAMs) of *n*-alkanethiolates SC_n (with n = number of carbon atoms) incorporated in junctions having structure Ag^{TS}-SAM//Ga_2O_3/EGaIn leads to a value for the injection tunnel current density J_0 (i.e., the current flowing through an ideal junction with $n = 0$) of $10^{3.6\pm0.3}$ A·cm^{-2} ($V = +0.5$ V). This estimation of J_0 does not involve an extrapolation in length, because it was possible to measure current densities across SAMs over the range of lengths $n = 1-18$. This value of J_0 is estimated under the assumption that values of the geometrical contact area equal the values of the effective electrical contact area. Detailed experimental analysis, however, indicates that the roughness of the Ga_2O_3 layer, and that of the Ag^{TS}-SAM, determine values of the effective electrical contact area that are $\sim10^{-4}$ the corresponding values of the geometrical contact area. Conversion of the values of geometrical contact area into the corresponding values of effective electrical contact area results in $J_0(+0.5\text{ V}) = 10^{7.6\pm0.8}$ A·cm^{-2}, which is compatible with values reported for junctions using top-electrodes of evaporated Au, and graphene, and also comparable with values of J_0 estimated from tunneling through single molecules. For these EGaIn-based junctions, the value of the tunneling decay factor β ($\beta = 0.75 \pm 0.02$ Å^{-1}; $\beta = 0.92 \pm 0.02$ nC^{-1}) falls within the consensus range across different types of junctions ($\beta = 0.73-0.89$ Å^{-1}; $\beta = 0.9-1.1$ nC^{-1}). A comparison of the characteristics of conical Ga_2O_3/EGaIn tips with the characteristics of other top-electrodes suggests that the EGaIn-based electrodes provide a particularly attractive technology for physical-organic studies of charge transport across SAMs.

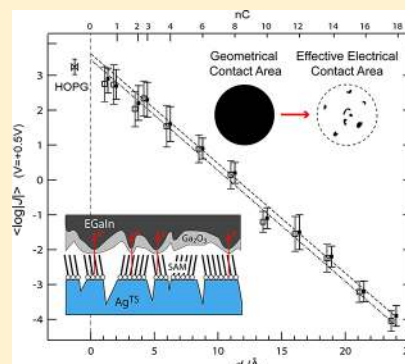

■ INTRODUCTION

Measurements, using a number of techniques, of rates of charge transport by tunneling across self-assembled monolayers (SAMs) of *n*-alkanethiolates on silver and gold substrates show an interesting, puzzling, and unresolved mixture of consistency and inconsistency. Rates of tunneling across these SAMs follow the simplified Simmons equation,[1,2]

$$J(V) = J_0(V) \times 10^{-\beta d/2.303} \tag{1}$$

with the falloff in current density $J(V)$ (A·cm^{-2}) with increasing length d of the *n*-alkyl group giving (for even-numbered carbon chains, and at voltages in the range $V = \pm0.5$ V) approximately the same value of the tunneling decay factor β by most or all methods of measurement ($\beta = 0.73-0.89$ Å^{-1}; for d = nC = number of carbon atoms, $\beta = 0.90-1.1$ nC^{-1}). Using mercury drops as top-electrodes, measurements of rates of tunneling across *n*-alkanes anchored to heavily doped silicon surfaces led to $\beta = 0.9 \pm 0.2$ nC^{-1}, similar to the values observed for *n*-alkanethiolates on Au and Ag substrates.[3,4]

By contrast, values of the injection current $J_0(V = +0.5\text{ V})$—the limiting value of current for an ideal junction with no hydrocarbon present ($d = 0$), but with all the interfaces and characteristics of junctions containing the SAMs—vary from $\sim10^8$ A·cm^{-2}, estimated from single-molecules approaches[5−10] and measured for graphene[11] and evaporated gold[12] top-electrodes, to $\sim10^2$ A·cm^{-2}, observed in large-area junctions using, as top-electrodes, conductive polymers,[13] Hg-drops supporting an insulating organic film (Hg-SAM),[14−16] and Ga_2O_3/EGaIn tips.[17−20] Why is there high consistency in values of β, but broad inconsistency in values of $J_0(V)$ within these systems?

A priori, at least four factors might contribute to differences in $J_0(V)$ among methods of measurements:

(i) In large-area junctions, assuming that the effective electrical contact area (A_{elec})—the area through which current actually passes—coincides with the geometrical contact area (A_{geo}) estimated by optical microscopy could result in errors in the conversions of values of current into current densities. Contact between surfaces occurs only through asperities distributed on the surfaces, which are always rough to some extent; in addition, only a fraction of the true, physical contact area is conductive.[21−24] Estimations of the effective contact area from measurements of adhesion and friction between surfaces indicate that values of A_{elec}/A_{geo} vary in the range $10^{-2}-10^{-4}$, depending on the hardness of the materials, the heights, widths, and number of asperities on both surfaces, and loads applied to the contacts.[22,23,25−27]

Received: August 20, 2013
Published: November 4, 2013

 © 2013 American Chemical Society dx.doi.org/10.1021/ja408652h | J. Am. Chem. Soc. 2013, 135, 18131−18144

(ii) The resistivities of the SAM//electrode contacts might vary due to the nature of the interactions at the top-interface (e.g., covalent bonding versus van der Waals contacts), to differences in the resistivities of the electrode materials, and to the presence of adsorbed insulating impurities.

(iii) The preparation of the top-electrode might damage the SAM (e.g., by reaction of hot metal atoms condensing on top of the SAM, by formation of metal filaments that partially or completely bridge the SAM,[28−30] and/or by displacing the SAM).

(iv) The range may also, to some extent, be an artifact: values of J_0 have often been determined by long extrapolations from small ranges of lengths and based on data characterized by large (and often not statistically determined) dispersions in measured values of current densities for individual *n*-alkanethiolates.

There has been much speculation about the relative importance of these factors, but there is little experimental evidence with which to decide among them. Review articles[31,32] have considered (approximately) that the electrical behavior of different types of junctions might be influenced by the bulk resistivities of the materials used for the top-electrodes. We observe, however, that correlation of the structures of the molecules making up the SAM with rates of charge transport through these molecules would be impossible if the electrical properties of the top-electrode were to dominate the behavior of the junctions. By contrast, the consensus on the value of β for tunneling across SAMs of *n*-alkanethiolates (β = 0.73−0.89 Å^{-1}; β = 0.9−1.1 nC^{-1}) strongly suggests that these junctions capture details that are characteristic of charge transport through molecules.

We[17,19,20,33−37] and others[38−40] have been developing Ga_2O_3/EGaIn soft top-electrodes to contact SAMs formed on template-stripped Au and Ag substrates. We have previously reported[41] that the layer (average thickness of ~0.7 nm in simple, mechanically unstressed systems) that spontaneously forms on the surface of EGaIn electrodes consists primarily of Ga_2O_3, and that this Ga_2O_3 layer is redox-inactive in the range $V = \pm 1$ V.[34,42] Two of the remaining areas that still need better definition are the effective area of electrical contact between the SAM and the Ga_2O_3/EGaIn top-electrode, and the resistance of the Ga_2O_3.

This paper reaches five major conclusions:

(i) In junctions using conical Ga_2O_3/EGaIn electrodes on top of SAMs formed on template-stripped silver substrates, the effective electrical contact area is ~10^{-4} the geometrical contact area (measured by optical microscopy).

(ii) The resistance of the Ga_2O_3 layer is lower than the resistance of the SAM of the shortest *n*-alkanethiolate (Ag^{TS}-S-CH_3) and makes no significant contribution to the resistance of the junction for any length of *n*-alkanethiolate group (Figure 1).

(iii) Flattening and stabilizing the surface of the Ga_2O_3/EGaIn tip reduces (by ~60%) the dispersion in values of log $|J(V)|$.

(iv) For junctions having the structure Ag^{TS}-SR//Ga_2O_3/EGaIn (Ag^{TS} = template-stripped silver substrate; R = C_nH_{2n+1}, with n = 0−18), $J_0 = 10^{3.6\pm0.3}$ A·cm^{-2} at V = +0.5 V. This value of J_0 is much more accurate than previous estimates, in part because we can measure tunneling currents through short-chain (n = 1−4) alkyl groups.

(v) Approximating the effective electrical contact area by the geometrical contact area leads to a significant overestimation of the electrical contact area and to an underestimation of the effective value of J_0. Correcting the value of J_0 determined experimentally by the estimated ratio $A_{elec}/A_{geo} = 10^{-4.0\pm0.5}$ gives $J_0 = 10^{7.6\pm0.8}$ A·cm^{-2} (V = +0.5 V); this correction reconciles the value of J_0 for Ag^{TS}-SAM//Ga_2O_3/EGaIn junctions with the values of J_0 reported for single-molecule approaches,[5−9] graphene,[11] and evaporated gold[12] electrodes (10^8−10^9 A·cm^2).

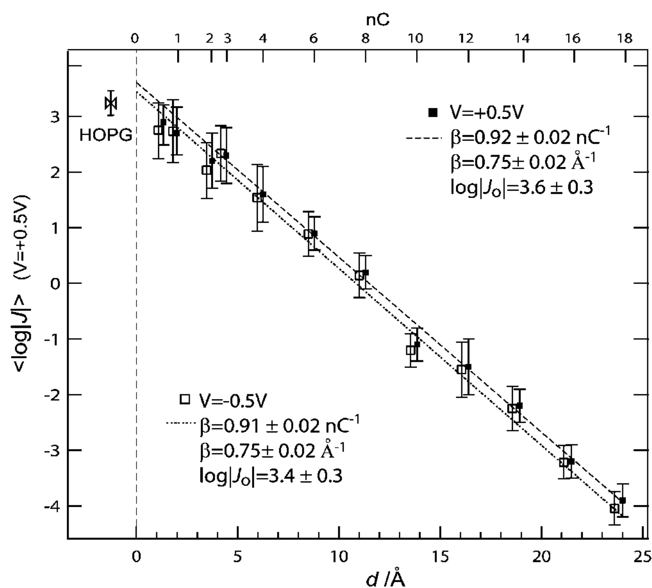

Figure 1. Plot of the Gaussian mean values ⟨log|J|⟩ through SAMs of *n*-alkanethiolates on Ag^{TS} substrates versus the length d of the tunnel gap established by the alkyl chain. Assuming a through-molecule tunneling, d was measured as the distance in Å from the S-terminus of the *n*-alkanethiolates (in their *all-trans* configuration) to the distal H atom closest to the top-electrode. On the top-axis, d is given as number of C atoms (nC) of the molecular backbone. Dashed lines represent the linear regression analyses, which give β/2.303 (slopes) and log$|J_0|$ (intercepts at d = 0). "HOPG" indicates the logarithm of the conductance of Ga_2O_3 estimated from charge transport across the HOPG//Ga_2O_3/EGaIn junction.

We emphasize that the correction of the electrical contact area has no influence on appropriately designed physical-organic studies, since these studies rely entirely on comparisons of tunneling currents across different organic groups for which the Ag^{TS}-SR and the SAM//Ga_2O_3 interfaces will have the same properties. Top-interfaces involving SAMs formed with different types of molecules, and with different electronic structures (e.g., Ag^{TS}-S-alkyl and Ag^{TS}-S-aromatic), may be different for various reasons. In this work, we thus assume that correction of the values of current density $J(V)$ for the effective electrical contact area is unnecessary for physical-organic studies comparing SAMs derived from HSC_n. For this type of studies, our estimation of J_0—a value that is particularly accurate because it does not involve the long extrapolation from n = 10−18 to n = 0 characteristic of most prior work—provides a reference value that can be used to test the quality of data for tunneling across *n*-alkanethiolates collected in different laboratories using conical Ga_2O_3/EGaIn tips.

BACKGROUND

Ga_2O_3/EGaIn as a Material for Top-Electrodes. We are developing liquid top-electrodes of eutectic gallium indium alloy (EGaIn) for studies of charge transport through SAMs. Upon exposure to air, EGaIn forms (essentially instantaneously

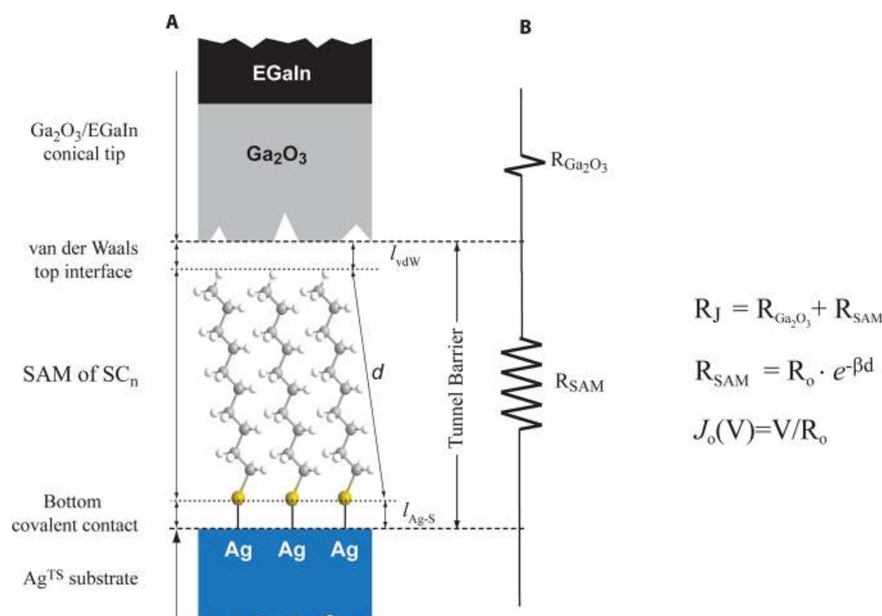

Figure 2. (A) Structure of Ag^{TS}-SAM//Ga_2O_3/EGaIn junctions. (B) Components of the resistance of the junction (R_J): R_{SAM}, tunneling resistance across the SAM; $R_{Ga_2O_3}$, resistance of the Ga_2O_3 layer; l_{Ag-S}, length of the bottom Ag^{TS}−S covalent contact; l_{vdW}, thickness of the top SAM//Ga_2O_3 van der Waals interface; d, length of the tunnel barrier established by the alkyl chain. Assuming a through-bond mechanism, d coincides with the length of the alkyl chain. J_0 is defined as the current across a junction with $d = 0$.

on the time scale of these experiments) a thin (nominally ∼0.7 nm[40]), self-passivating oxide layer (mostly Ga_2O_3).[41,43] This layer, although mechanically fragile, enables us to fabricate geometrically defined tips.[44] During fabrication, and in contacting the SAM, it buckles, and this buckling generates rough Ga_2O_3 surfaces.

For most of our work, we have used Ga_2O_3/EGaIn conical tips as top-electrodes for five reasons: (i) They can (partially) adapt to the topography of the substrate. (ii) They are particularly convenient to use in physical-organic studies, which require trends in $J(V)$ with the structure of the SAM rather than absolute values of $J(V)$. (iii) They appear not to damage the SAM. (vi) They do not require expensive hardware or sophisticated equipment to generate reproducible data. (v) They make it possible to collect large numbers of data (∼10^3 complete J−V sweeps per day); these numbers provide the basis for detailed statistical analyses of uncertainty, dispersion, and variability of values. We point out that many of the results for molecular tunneling described in the earlier literature appear to rely on single, selected data points, or small numbers of points, and are literally uninterpretable because they do not distinguish between statistically defined values (means based on large numbers of data) and outliers or artifacts (which may be displaced many orders of magnitude from the mean).[18,45]

Electrical Structure of the Ag^{TS}-SAM//Ga_2O_3/EGaIn Junction. For a fixed voltage, we can consider junctions having structure Ag^{TS}-SAM//Ga_2O_3/EGaIn as being two resistors in series (Figure 2): the Ga_2O_3 layer, with specific resistance $R_{Ga_2O_3}$, and the tunnel gap established by the SAM, which has specific resistance R_{SAM}. This tunnel gap extends from the surface of the Ag^{TS} bottom-substrate to the surface of the Ga_2O_3 layer of the top-electrode. The resistance of the junction is thus given by

$$R_J = R_{SAM} + R_{Ga_2O_3} \quad (2)$$

The tunneling resistance R_{SAM} originates, in principle, from three components (Figure 2): (i) the resistance of the van der Waals top-interface, which has thickness l_{vdW}; (ii) the resistance of the tunneling barrier established by the alkyl chain (for a through-molecule transport, the length d of this tunnel barrier is given by the length of the alkyl chain); and (iii) the resistance of the Ag−S covalent contact, whose length is l_{Ag-S}. Adopting, for these three components, the formalism of the Simmons model, the resistance of the tunnel gap can be (formally) written as

$$R_{SAM} = R_0^{o}\, e^{-\beta_{vdW} l_{vdW}}\, e^{-\beta_{Ag-S} l_{Ag-S}}\, e^{-\beta d} \quad (3)$$

In eq 3, R_0^o accounts for the electronic properties of the surfaces of the Ag^{TS} substrate and of the Ga_2O_3 layer; β_{Ag-S} and β_{vdW} are the hypothetical decay factors for tunneling across the Ag−S and the SAM//Ga_2O_3 van der Waals interface, respectively; and β is the tunneling decay factor characteristic of n-alkanes.

If $R_{Ga_2O_3} \ll R_{SAM}$, the electrical behavior of the junction is dominated by tunneling across the SAM ($R_J \approx R_{SAM}$), and trends in $J(V)$ with the structure of the molecules in the SAM will be useful in understanding the relationship between molecular structures and tunneling rates. If, however, the resistance of the Ga_2O_3 were similar to ($R_{Ga_2O_3} \approx R_{SAM}$) or larger than ($R_{Ga_2O_3} > R_{SAM}$) that of the SAM, interpretation of data for charge transport through SAMs could be difficult or impossible.

In a previous study,[34] our group estimated a value of the specific resistance (i.e., the resistance per unit area) of the Ga_2O_3 layer as $R_{Ga_2O_3} \approx 4 \times 10^{-2}$ Ω·cm^2. This value of $R_{Ga_2O_3}$ was ∼10^4 times lower than that of a SAM composed of SC_9, the shortest molecule studied at that time.[19] We thus concluded that, for medium-length SAMs (n = 9−18), the values of $J(V)$ were determined by the SAM; this inference did not automatically apply to short-chain SAMs (which were not examined in previous studies). In this work, we correct this

Table 1. Comparison of Values of Injection Tunnel Current $J_0(V = +0.5\ \text{V})$ and Tunnel Decay Factor β for *n*-Alkanethiolates (SC_n) Reported (or Estimated) for Different Types of Junctions

type of junction	top-electrode	bottom-electrode	values of *n*	$\log\|J_0\|$ (J_0/A·cm^{-2})	β (nC^{-1})	ref
Au-SAM//polymer/Hg[a]	conductive polymer	as-dep[e]	8, 10, 12, 14, 16	~2	1.10 ± 0.04	13
Ag-SAM//Ga_2O_3/EGaIn	Ga_2O_3/EGaIn (cone)	TS[f]	9, 11, 13, 15, 17	1.9	1.00 ± 0.02	18
Ag-SAM//Ga_2O_3/EGaIn	Ga_2O_3/EGaIn (cross-bar)	TS	12, 14, 16, 18	~2.5	0.95 ± 0.2	20
Ag-SAM//Ga_2O_3/EGaIn	Ga_2O_3/EGaIn (cone)	TS	10, 12, 14, 16, 18	2.5	0.97 ± 0.02	18
Ag-SAM//Ga_2O_3/EGaIn	Ga_2O_3/EGaIn (cone)	TS	10, 12, 14, 16	~3	1.1 ± 0.2	19
Ag-SAM//Ga_2O_3/EGaIn	Ga_2O_3/EGaIn (cone)	TS	0–18	3.6 ± 0.3	0.92 ± 0.02	this
Ag-SAM//SAM-Hg[b]	Hg-SC_{16}	as-dep	8, 10, 12, 14, 16	~3	1.0	15
Au-SAM-Au	Au nanoskiving	nanoskiving	12, 14, 16	3.2	0.94	51
Au-SAM//PEDOT/Au	PEDOT:PSS	as-dep	8, 10, 12, 14	~5	0.76	47
Hg-SAM//SAM-Hg[c]	Hg	liquid metal	18, 20, 22, 24, 28	~6	0.9	50
Hg-SAM//Hg[d]	Hg	liquid metal	9–12, 15, 16, 18	~6	1.04 ± 0.07	49
nSi-SAM//Hg	Hg	n-Si[g]	14, 16, 18	6.5[h]	0.9 ± 0.2	3, 4
Au-SAM//graphene	graphene	TS	8, 12, 16	8.3	1.02 ± 0.1	11
Au-SAM-Au	Au evaporated	TS	8, 12, 16	~8	0.98 ± 0.03	12
Au-SAM-Au	STM tip	single crystal[i]	6, 8, 10	8.9	1.09	5–7
Au-SAM-Au	AFM tip	single crystal	6, 8, 10, 12	8.2	0.8	8, 9

[a]Conductive polymer = polyphenylenevinylene-type polymer. [b]J_0 extrapolated at the length of the top-SAM. Including the top-SAM in the tunnel barrier of the junction yields $\log|J_0| \approx 6$. [c]J_0 not reported by the authors of the original paper; we estimated J_0 from published data. [d]Junction held under electrochemical control. [e]as-dep = as-deposited, rough metal substrate. [f]TS = template-stripped, flat metal substrate. [g]Highly n-doped silicon. [h]J_0 calculated from contact conductance of a single molecule reported in the original article. [i]Flat terraces of single-crystal surfaces.

value to $R_{Ga_2O_3} = 3.3 \times 10^{-4}\ \Omega\cdot\text{cm}^2$; this change does not alter our understanding of the junction.

Properties of the SAM//Ga_2O_3/EGaIn Top-Contact, and Sources of Uncertainty. The Ga_2O_3/EGaIn top-electrode is in van der Waals contact with SAMs of *n*-alkanethiolates, which terminate in CH_3 groups. Because the formation and manipulation of conical tips generate a Ga_2O_3 layer that is variable in thickness, and that further buckles and unfolds during manipulation, the surface of the top-electrode is rough. The surface of the Ag^{TS} substrate, and thus the topography of the top-surface of the SAM, is also rough (due to steps, grain boundaries, and other defects in the silver surface, and to irregularities in the order and structure of the SAM[46]). This heterogeneity in structure, topography, and thickness results in an effective electrical contact area that is smaller than the area of the geometrical contact estimated by microscopy.

In addition to the heterogeneities in the Ga_2O_3 film, other factors that can contribute to uncertainties in data collected with Ga_2O_3/EGaIn top-electrodes include (i) the presence of adventitious contaminants adsorbed on the tip and/or the SAM (although a methyl-terminated surface has a low interfacial free energy and a low tendency to adsorb impurities, metals and metal oxides have high surface energies) and (ii) the formation of conductive filaments between the top-electrode and the metal substrate.[28–30]

Charge Transport across SAMs. The Simmons model[1,2] provides an approximate analytical equation (eq 1) for charge tunneling through a potential barrier established by an organic insulator; in this model, the value of the decay factor β is determined by the height of the potential barrier. Currently, no molecular theory correlates experimental values of $J(V)$ and β with molecular structure, and the Simmons model may be inappropriate and incomplete[47,48] (especially for organic SAMs more complicated than simple *n*-alkanes, or when these SAMs involve electronically conductive regions, although we observed that charge transport across a variety of complex structures is very similar to tunneling through *n*-alkanethiolates[37]). Nonetheless, in the absence of a more developed theory, the simplified Simmons equation has been adopted as the theoretical standard for analyses in studies of charge tunneling across organic molecules because, in the low-bias regime, it reduces the tunneling problem to the determination of just two parameters: β and J_0.

Values of J_0 for tunneling across *n*-alkanethiolates estimated by different techniques differ by more than 10^7 A·cm^{-2}; these techniques use a variety of different top-electrodes, which include Hg-drops,[49] Hg-SC_nSCH_3[14–16,50] (that is, Hg-drops supporting a monolayer of $S(CH_2)_nCH_3$, with $n = 11, 13, 15$), conductive polymers,[13,47] Ga_2O_3/EGaIn[18–20] tips, evaporated Au electrodes,[12] Au electrodes fabricated via nanoskiving,[51] graphene,[11] and scanning tunneling microscopy (STM)[5–7] and atomic force microscopy (AFM)[8,9] tips. Table 1 summarizes values of $J_0(V = +0.5\ \text{V})$ reported or estimated for these junctions.

Experiments with different junctions using the same material for the top-electrode have given substantial differences in J_0; this variability is in contradiction with theory and intuition, both of which would predict that the same materials would give the same values of $J_0(V)$. Our hypothesis is that differences in J_0 arise from differences in the procedures used to fabricate the top-electrode, rather than from differences in materials. Junctions using Au electrodes directly evaporated[12] on top of the SAM yielded a value of J_0 (10^8 A·cm^{-2}) that was 10^5 that reported for junctions using Au top-electrodes fabricated via nanoskiving[51] ($J_0 = 10^{3.2}$ A·cm^{-2}). We believe both values are correct, but specific to different experiments. The different behavior probably reflects differences in the values of A_{elec}/A_{geo} due to differences in the roughness of the electrodes.

Using highly conductive polyphenylenevinylene layers[13] and Hg-drops carrying an organic insulator[15] as top-contacts on SAMs formed on rough (as-evaporated) substrates yielded values of J_0 (10^2–10^3 A·cm^{-2}) close to the values of J_0 obtained using highly conductive, but rough, Ga_2O_3/EGaIn conical tips.[18,20] By contrast, values of $J_0 \approx 10^8$ A·cm^{-2} are reported for large-area junctions using flat metal substrates and flat (e.g., graphene[11]) or conformal (e.g., evaporated Au[12]) top-electro-

des; these values of $J_0(V)$ are close to those estimated from single-molecule techniques (~10^8–10^9 A·cm^{-2}).

For junctions using Hg-drops on top of alkyl chains anchored to heavily doped Si surfaces, Cahen and co-workers reported a value of $J_0 \approx 10^{6.5}$ A·cm^{-2} for p-Si substrates,[4] and a value of $J_0 \approx 10^4$ A·cm^{-2} for n-Si substrates[48] (we estimated these values of J_0 from data reported by the authors[4,48]). For the system with $J_0 \approx 10^4$ A·cm^{-2}, however, fitting the Simmons equation to experimental J–V curves for individual n-alkanes required a correction of the contact area by a factor of ~10^{-4} in order to get meaningful fitting parameters[3] (30 μm^2 contact area required by the fitting, over a geometrical contact area of 5 × 10^4 μm^2); Cahen et al. argued that theoretical modeling of experimental tunneling rates characterized by $J_0 \leq 10^4$ A·cm^{-2} "may lack physical relevance".[3]

These results indicate that different properties (we believe primarily topographies of the surfaces) of top- and bottom-electrodes—and not the resistances of the corresponding bulk materials—determine the spread of the experimental values of J_0 across different methods (Table 1).

■ EXPERIMENTAL DESIGN

SAMs of *n*-Alkanethiolates with Even Numbers of Carbon Atoms. *n*-Alkanethiols ($CH_3(CH_2)_{n-1}SH$, represented here as SC_n) are commercially available in a range of lengths; they are accepted as the simplest model system for physical-organic studies of tunneling through SAMs. (We note that the complexity of structural features of SAMs of *n*-alkyl chains—e.g., packing density, insoluble multilayer metal thiolate "soaps" for silver, defects, roughness of the underlying metal—makes these SAMs more complex than they first seem.[52]) We collected J–V data for SAMs composed of SC_n with even numbers of carbons from n = 2 to n = 18. We excluded long (n > 5) *n*-alkanethiolates with odd numbers of carbons because they behave differently from those with even n, and require a separate analysis.[14,19]

Measurements on Short *n*-Alkanethiolates with Odd Numbers of Carbon Atoms. In order to study the frequency of the failure of the junctions, and to provide values of $J(V)$ for SAMs composed of short molecules, we measured rates of charge transport through SAMs formed from CH_3SH (SC_1), and $CH_3(CH_2)_2SH$ (SC_3), and through Ag^{TS}-SH (SC_0). (We formed CH_3SH and H_2S by hydrolysis of CH_3SNa and Na_2S, respectively.) We describe experimental details of the preparation of the SAMs in the Supporting Information.

Template-Stripped Substrates. We formed SAMs on template-stripped Ag (Ag^{TS}) substrates.[19,46] Template stripping provides surfaces characterized by large flat terraces (average area of terraces ~0.13 μm^2). Template-stripped surfaces give larger effective electrical contact areas than "as-evaporated" top-surfaces;[46] the value of A_{elec}/A_{geo} is, however, limited by the roughness of the terraces, by the size of the silver grains, and by the width and the depth of grooves between grains. Forming SAMs on silver template-stripped substrates yielded ~90% of nonshorting junctions.

Fabrication of Flattened Conical Tips, and Formation of Stable Contacts on Top of the SAM. The apparent non-Newtonian properties of the Ga_2O_3/EGaIn[43] enable several procedures for the fabrication of the top-electrode. For this paper, we used what we call "flattened" conical tips. Although these tips are characterized by an effective electrical contact area that we know to be less than the nominal contact area we measure by optical microscopy, they can be quickly and easily fabricated and used in physical-organic studies, where convenience and the ability to generate large number of data are more important in correlating different molecular systems with values of $J(V)$ than is high precision (this type of use assumes, of course, that $J_0(V)$ is the same across all the junctions formed with different tips). Figure 3 summarizes the five steps of the procedure we used to fabricate flattened conical tips: (1) We extruded a Ga_2O_3/EGaIn drop from a 10-μL syringe. (In order to keep the weight of the EGaIn column constant in all junctions, we always used 2 μL of EGaIn.) (2)

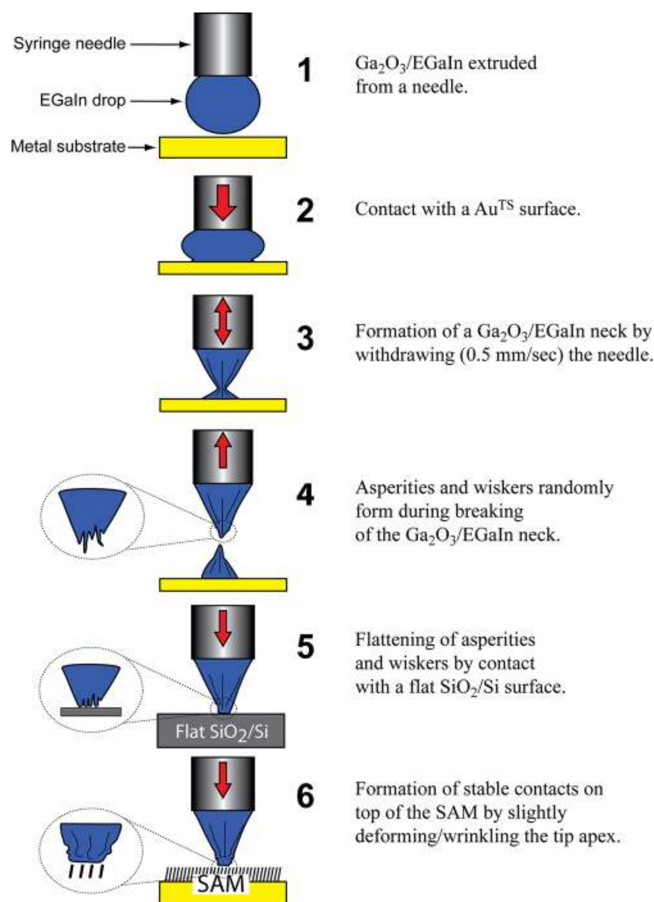

Figure 3. Procedure for the fabrication of flattened Ga_2O_3/EGaIn conical tips. Flattening is achieved by contact of the tip with a flat Si/SiO_2 surface (step 5). In step 4, the sizes of asperities are exaggerated for clarity. A video of this procedure is available as Supporting Information.

With a micromanipulator, we brought the Ga_2O_3/EGaIn drop in contact with a clean metal substrate (usually Au^{TS}). (3) We slowly (~0.5 mm/s) pulled the syringe away from the surface to form a Ga_2O_3/EGaIn neck. (4) By further withdrawing the syringe, we broke the Ga_2O_3/EGaIn neck and obtained a top-conical tip. The surface of this as-fabricated conical tip is characterized by asperities and whiskers randomly formed while forming and breaking the neck. Analysis of data collected with these tips revealed that an important source of dispersion in the measured values of $J(V)$ was the variation of these values from junction to junction, probably due to the progressive deformation of asperities (Supporting Information, Figure S1). (5) We flattened the asperities of the as-fabricated conical tip by touching it three times to a flat, polished SiO_2/Si surface (the type of SiO_2/Si substrates used for template-stripped metal surfaces). We observed that this procedure stiffened the tip and led to more stable contacts. We also observed that running three cyclic voltage scans between ±2 V while the tip is in contact with the Si chip further reduced the dispersion in data for J.

We used the flattened conical tips as top-electrodes on Ag^{TS}-SAM substrates (Figure 3, step 6). To form stable contacts, we brought the tips closer to the substrates until we could clearly observe (by optical microscopy) the tip apex wrinkling, or deforming; from this point, current densities did not change for applied forces varying in the range 2–4 g·cm^{-2}. (We thus used the "wrinkling" of the Ga_2O_3 skin on the sides of the conical tip as an indication of the load applied.) We did not explore larger deformation of the tips.

This procedure for the fabrication of flattened tips, and for the formation of stable contacts on top of the SAMs, generated reproducible values of $J_0(V)$, β, and σ_{log} among different users. The

standard deviations of values of log|J| measured with these flattened conical tips were by 60% smaller than those observed for as-fabricated tips; flattening the tip, however, had no effect on ⟨log|J|⟩, the mean values of the distributions (Supporting Information, Figure S1). A video of the fabrication of a flattened conical tip is available as Supporting Information.

Protocol for Collection of Data. We have observed that data collected with an unstandardized protocol (that is, forming an arbitrary number of junctions, running arbitrary numbers of scans) can broaden data distributions. We have thus introduced a standard procedure for data acquisition, which we call the "1/3/20" protocol. For each individual tip, we formed three junctions (i.e., contacts) in three different places of the Ag^{TS}-SAM; for each junction, we recorded 20 J–V traces for forward bias (V = −0.5 V → V = +0.5 V) and 20 $J(V)$ traces for reverse bias (V = +0.5 V → V = −0.5 V). From empirical comparison of procedures, we speculate that, by limiting the number of junctions per tip, the 1/3/20 protocol may avoid collecting data with EGaIn tips contaminated by adventitious impurities. Collecting the same number of data per tip (120 points in total) ensures that all tips have the same statistical weight.

The 20 scans are necessary so that we do not statistically overweight instabilities of the current that often occur during the first scans of a junction.[18] Collecting more than five scans per junction, however, produces autocorrelated data,[18] but this autocorrelation has no influence on the mean values and dispersions of our data sets, because it arises mainly from redundant data.[18]

Definition of the Tunnel Injection Current Density $J_0(V)$. In this paper, we define the injection current $J_0(V)$ for Ag^{TS}-SC_n//Ga_2O_3/EGaIn junctions as the value of $J(V)$ given by eq 3 for d = 0, that is, the value of $J(V)$ for an ideal junction with no alkyl chain, but with all characteristics and interfaces of junctions containing the SAM:

$$J_0(V) = V/(R_0^\circ\, e^{-\beta_{vdW} d_{vdW}}\, e^{-\beta_{Ag-S} d_{Ag-S}}) \equiv V/R_0 \tag{4}$$

We adopted this definition of $J_0(V)$ for two reasons:

(1) The value of $J_0(V)$ given by eq 4 can be easily estimated by extrapolating to d = 0 values of log|$J(V)$| for n-alkanethiolates of different lengths. The extrapolation requires that values of log|$J(V)$| decay with a constant slope (that is, constant β) along the full range of lengths. We recall that the tunnel barrier also includes the Ag−S and SAM//Ga_2O_3 van der Waals interfaces. But the β factors of the top- and bottom-interfaces are unknown; assuming that the interfaces have the same β as the alkyl chain might lead to errors in the estimation of the value of J_0 (this error might be significant for SAMs formed using anchoring group longer than Ag−S, for example, C≡C—R or O_2C—R[53]).

(2) Defining $J_0(V)$ for d = 0 gives a value of injection current that incorporates the rates for charge transport across the top- and bottom-interfaces (eq 4). This value of $J_0(V)$ can be used to compare the efficiency of charge injection into thiolates with that into other anchoring groups (provided that for these other anchoring groups d = 0 is defined on the first atom to which the alkyl chain is bound, and that the van der Waals top-interface remains unchanged); alternatively, values of $J_0(V)$ for SAMs of n-alkanethiolates having different terminal groups can be used to compare the efficiencies of charge injections into van der Waals top-interfaces having different structures.

We point out that the value of J_0 given by eq 4 varies linearly with the applied voltage (that is, constant value of R_0) only in the range of voltages −0.1 V ≤ V ≤ +0.1 V.[20] Assuming, however, that for a fixed voltage the value of R_0 is invariant across SAMs of different n-alkanethiolates, in this paper we estimate the value of J_0 for the applied voltage V = +0.5 V (and V = −0.5). At V = +0.5 V, rates of charge tunneling follow (qualitatively) the Simmons equation (eq 1); in addition, values of tunneling current across SAMs of the full set of n-alkanethiolates (SC_n, with n = 1−18) fall within the operative range of our electrometer (105 mA to 0.1 nA). At voltages > +0.5 V (< −0.5 V), resonances of the Fermi levels of the electrodes with molecular or interfacial electronic states lead to nonlinear variation of J_0 with V,[54] and the approximate Simmons equation does not describe charge tunneling adequately. In this paper we do not explore the high-bias regime.

Assuming a through-molecule tunneling, we measure the thickness d of the tunnel barrier established by the n-alkyl chains as the distance in angstroms from the S-terminus of the n-alknethiolates to the distal hydrogen atom closest to the top-electrode (Figure 2). To compare our results with others reported in the literature, we also estimated d as the number of C atoms (nC) of the alkyl backbone. We observe, however, that the length of the molecules as nC does not take into account the contribution of the length of the distal C−H bond(s) to the width of the tunneling barrier generated by *trans*-extended n-alkanethiolates (Figure S2), and thus leads to a systematic underestimation of the extrapolated value of J_0. In addition, giving d as nC might also lead to apparent inconsistencies between the electrical behavior of alkyl chains with odd and even number of C, because, due to the tilt angle of the SAM, the orientation of the distal C−H bond (and thus the effective length of the tunnel barrier) differs for these two classes of n-alkanethiolates (Figure S2). It is also evident that the comparison of the electrical behavior of SAMs of n-alkanethiolates with those of SAMs composed of molecules having different structure (e.g., SAMs of aromatic molecules) requires that d be given in Å.

Statistical Analysis of Data for Current Density across SAMs. We estimated J_0 ($A \cdot cm^{-2}$) and β ($Å^{-1}$; nC^{-1}) by least-squares linear regression analysis of values of ⟨log|J|⟩ versus the width d of the tunnel barrier established by the n-alkanethiolates, which we assume to be in their *all-trans* configuration; ⟨log|J|⟩ is the Gaussian mean value of data for log|J|, where J is the current density (measured in $A \cdot cm^{-2}$ at V = +0.5 V, and defined for the geometrical contact area estimated by optical microscopy) through SAMs.

Because experimental data for log|J| are approximately normally distributed for all SAMs, we extracted mean values (⟨log|J|⟩) and standard deviations (σ_{log}) from Gaussian fits (calculated with standard least-squares fitting[18]) to histograms of data.

Estimation of the Specific Resistance of Ga_2O_3/EGaIn Tips. We estimated the apparent (that is, not corrected for the effective electrical contact area) specific resistance $R_{Ga_2O_3}$ (the resistance per unit area, $\Omega \cdot cm^2$) of the Ga_2O_3/EGaIn conical tips from the specific resistance of junctions with structure HOPG//Ga_2O_3/EGaIn (HOPG = highly ordered pyrolytic graphite). Because both HOPG and bulk EGaIn are highly conductive materials ($\rho < 10^{-6}\ \Omega \cdot cm$), the resistance of these junctions is dominated by the resistance of the Ga_2O_3 layer. The advantages of using HOPG surfaces in measurements of contact conductance are that (i) they provide ultraflat substrates with sub-nanometer roughness, (ii) they do not oxidize in air, and (iii) they can be easily regenerated before each experiment.

Estimation of the Effective Electrical Contact Area in Ag^{TS}-SAM//Ga_2O_3/EGaIn Conical Tip Junctions. We define the ratio of the effective electrical contact area (A_{elec}) to the geometrical contact area estimated by optical microscopy (A_{geo}) as

$$\frac{A_{elec}}{A_{geo}} = \alpha_{tip}\alpha_{SAM} \tag{5}$$

where α_{tip} and α_{SAM} are the fractions of the geometrical surface areas that are available for contact respectively in Ga_2O_3/EGaIn conical tips and in Ag^{TS}-SAM substrates; these fractions are defined as the ratios of the effective electrical contact areas to the geometrical contact areas of conical tips (α_{tip}), and Ag^{TS}-SAM (α_{SAM}) in contact with an ideally flat electrode (that is, an ideal electrode with a surface topography that does not reduce the effective electrical contact area). We estimated α_{tip} and α_{SAM} separately.

Estimation of the Fraction of the Geometrical Surface Area of Conical Tips Available for Contact (α_{tip}). We estimated α_{tip} as the ratio of the current density J_{tip} flowing through Ga_2O_3/EGaIn-conical tips, to the current density J_{Hg} yielded by Hg-drop electrodes, in junctions formed with a standard substrate. We assume that Hg-drop electrodes have smooth, conformal surfaces with an area available for contact close to the geometrical surface area ($\alpha_{Hg} \approx 1$). We used Fe^{TS}/Fe_2O_3 (Fe^{TS} = template-stripped iron substrate) as standard substrate because it does not amalgamate with Hg. We grew the Fe_2O_3

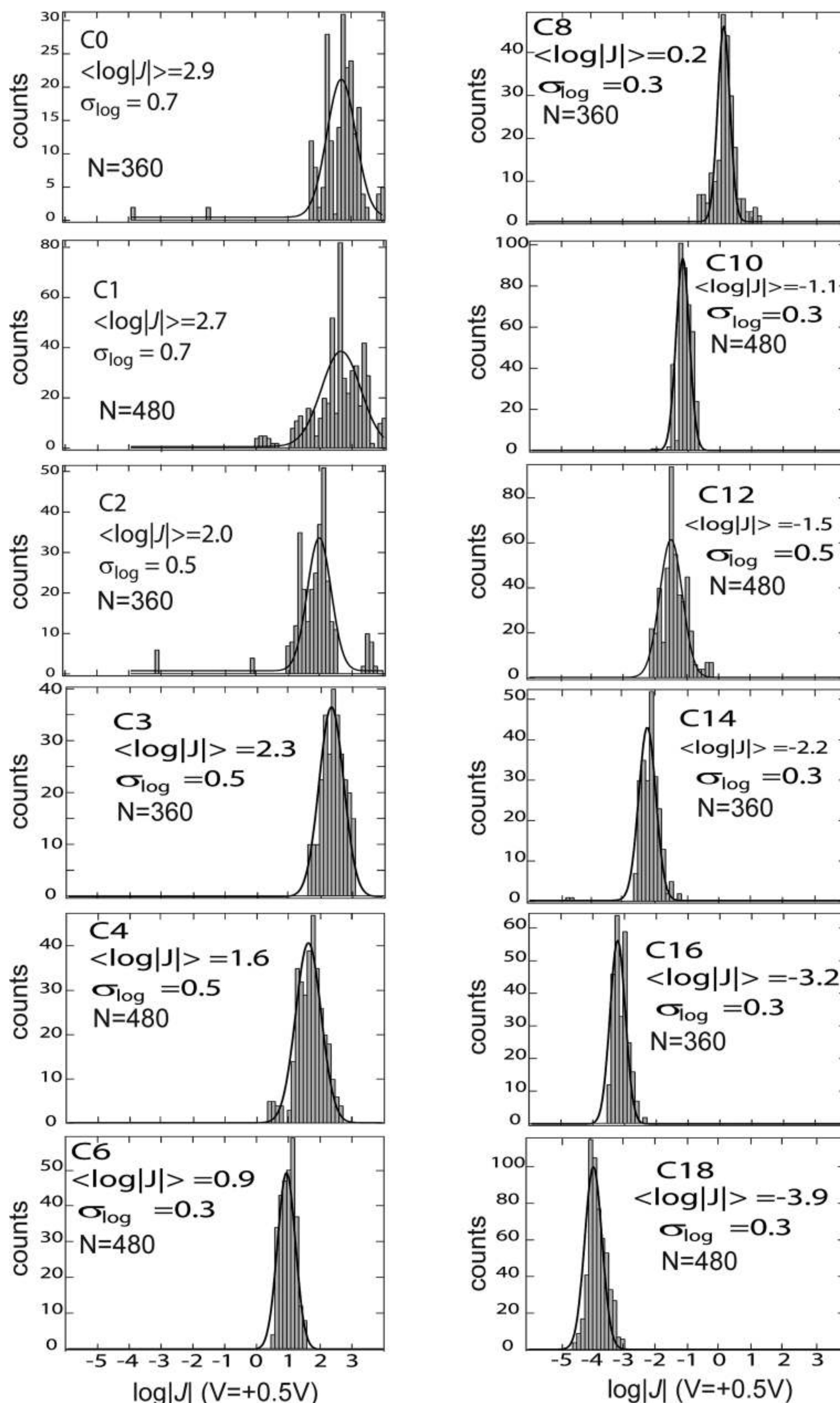

Figure 4. Histograms showing the distributions of values of log|*J*| at *V* = +0.5 V across Ag^{TS}-SAM//Ga_2O_3/EGaIn junctions using flattened conical tips. With "C*n*" we indicate SAMs of *n*-alkanethiolates with *n* carbon atoms. Solid curves represent Gaussian fits. *N* is the number of data points. Data were collected using the 1/3/20 protocol; no data were excluded. The heights of the bars of the histograms count the number of points (counts) with values of log|*J*| within the width (0.13) of the bars. For each distribution, the values of the Gaussian mean, median, and mode (the value of log|*J*| with the highest bar) differed by <0.1.

layer thermally with a specific resistance ($R_{Fe_2O_3} \approx 10\ \Omega\cdot cm^2$) that was $\sim 10^4$ higher than the apparent specific resistance of the Ga_2O_3 layer estimated using HOPG ($R_{Ga_2O_3} = 3.3 \times 10^{-4}\ \Omega\cdot cm^2$). Because $R_{Ga_2O_3} \ll R_{Fe_2O_3}$ by experimental design, the specific resistances of both Ga_2O_3/EGaIn and Hg-drop-based junctions are determined by $R_{Fe_2O_3}$, and, at a given voltage V, they must give the same effective current densities:

$$\frac{I_{tip}}{A_{tip}} = \frac{V}{R_{Fe_2O_3}} = \frac{I_{Hg}}{A_{Hg}} \quad (6)$$

In eq 6, I_{tip} is the current flowing through the effective electrical contact area A_{tip} in junctions using Ga_2O_3/EGaIn conical tips, and I_{Hg} is the current through the effective electrical contact area A_{Hg} in junctions using Hg-drops.

We define the effective electrical contact area for $Fe^{TS}/Fe_2O_3//Ga_2O_3$/EGaIn junctions as $A_{tip} = A_{geo,tip}\alpha_{tip}\alpha_{Fe_2O_3}$, where $A_{geo,tip}$ is the geometrical contact area of Ga_2O_3/EGaIn conical tips on the Fe_2O_3 substrate. Analogously, we define the effective electrical contact area of Fe^{TS}/Fe_2O_3//Hg junctions as $A_{Hg} = A_{geo,Hg}\alpha_{Fe_2O_3}$, with $A_{geo,Hg}$ being the geometrical contact area of Hg-drops on the Fe_2O_3 substrate. The fraction $\alpha_{Fe_2O_3}$ quantifies the contribution of the roughness of the Fe_2O_3 layer to the effective contact area. Equation 6 thus becomes

$$\frac{I_{tip}}{A_{geo,tip}\alpha_{tip}\alpha_{Fe_2O_3}} = \frac{V}{R_{Fe_2O_3}} = \frac{I_{Hg}}{A_{geo,Hg}\alpha_{Fe_2O_3}} \quad (7)$$

The fraction $\alpha_{Fe_2O_3}$ was the same for both junctions because we used the same Fe^{TS}/Fe_2O_3 chip for all measurements. We thus obtain

$$\frac{I_{tip}}{A_{geo,tip}\alpha_{tip}} = \frac{V}{R_{Fe_2O_3}} = \frac{I_{Hg}}{A_{geo,Hg}} \quad (8)$$

Experimental current densities, however, are calculated for the geometrical contact areas, that is,

$$J_{tip} = \frac{I_{tip}}{A_{geo,tip}} \text{ and } J_{Hg} = \frac{I_{Hg}}{A_{geo,Hg}} \quad (9)$$

Here, J_{tip} is the experimental current density for junctions formed with Ga_2O_3/EGaIn tips, and J_{Hg} is the experimental current density for junctions formed with Hg-drop junctions. By substituting eq 9 into eq 8, we obtain

$$\alpha_{tip} = \frac{J_{tip}}{J_{Hg}} \quad (10)$$

We estimated J_{tip} and J_{Hg} as mean values $\langle J_{tip}\rangle$ and $\langle J_{Hg}\rangle$ of data for current density at $V = +0.5$ V—collected following the 1/3/20 protocol—for $Fe^{TS}/Fe_2O_3//Ga_2O_3$/EGaIn conical tips, and for Fe^{TS}/Fe_2O_3//Hg-drop junctions.

Estimation of the Fraction of the Geometrical Surface of Ag^{TS}-SAM Substrates Available for Contact (α_{SAM}). We estimated α_{SAM} from digital analysis of a STM image of a Ag^{TS}-SAM substrate using

$$\alpha_{SAM} = \frac{q}{Q} \quad (11)$$

where q is the number of pixels within 2 Å from the top-most average plane of the digital image, and Q is the total number of pixels. The length used (2 Å) represents the variation of the length of the tunnel gap (±1.0 Å, that is, $\sim \pm\sigma_{log}$) calculated from the average standard deviation of log|J| ($\sigma_{log} = 0.3$) considering $\beta = 0.75$ Å^{-1} for n-alkanethiolates. We used a 900 nm × 900 nm STM image of a Ag^{TS}-SC_{10} substrate that did not present valleys or asperities that would require, for the estimation of α_{SAM}, that we take into account the partial adaptation of the Ga_2O_3/EGaIn tip to the topography of the surface.

RESULTS AND DISCUSSION

The yield of working junction is independent of the length of the molecule. We observed an average yield of working junction of ∼90% for all chain lengths (including n = 0). For the first time, we have been able to measure charge transport through SAMs composed of short molecules of SC_n (n = 0−6); the yields of working junctions for these short SAMs were approximately the same as those for the longer ones (n = 8 to n = 18). Yields of working junctions for individual n-alkanethiolates are summarized in Table S1.

The high yield observed for the very thin SAMs (n = 1−4) implies that junctions using Ga_2O_3/EGaIn junctions can sustain electric fields as high as 1 GV·m^{-1}. In a previous work,[55] we reported that junctions formed with Hg-drops broke down at electric fields ∼0.8 GV·m^{-1}. These results suggest that the breakdown electric field might be influenced by the mechanical properties (e.g., stiffness, rigidity) of the top-electrode, or by the resistance to lateral spreading under electrostrictive pressure of the SAM on Ag^{TS} (as opposed to Hg[56]). Junctions using solid, conductive AFM tips as top-electrodes can sustain electric fields as high as 3 GV·m^{-1}; as such, they are used in studies of charge transport at applied voltages >2 V.[57]

Statistical Analysis of Data for log|J|. Figure 4 summarizes histograms of data for log|J| (at V = +0.5 V) for SAMs of n-alkanethiolates from SC_0 to SC_{18} formed on Ag^{TS}. These histograms approximately fitted Gaussian curves, from which we extracted the mean values ⟨log|J|⟩ and standard deviations σ_{log}. For all molecules, Gaussian mean, median, and mode (the value of log|J| with the highest frequency) differed by <0.1. Statistical analysis of histograms for log|J| at V = −0.5 V (summarized in Figure S3) led to mean values ⟨log|J|⟩ and standard deviation σ_{log} similar to those obtained for V = +0.5 V, revealing a symmetry of tunneling rates in the range of voltages V = ±0.5 V. The Gaussian fits yielded values of $\sigma_{log} \approx 0.3$ (which corresponds to values of $J(V)$ from $0.5\times J(V)$ to $2\times J(V)$) for SAMs of long molecules (SC_6−SC_{18}), and an average value of $\sigma_{log} \approx 0.7$ (that is, values of $J(V)$ between $0.2\times J(V)$ and $5\times J(V)$) for SAMs of the short n-alkanethiolates (SC_1−SC_4). The difference in the value of σ_{log} between short and long molecules might be caused by a different structure of the SAM. SAMs of n-alkanethiolate with n < 5 are believed to have disordered, liquid-like structure, whereas long molecules form compact, crystalline films.[52]

Calculating J_0 and β. Figure 1 shows that values of ⟨log|J|⟩ (at both V = +0.5 and −0.5 V) decreased linearly with the length d of the S-$(CH_2)_n$-H group (d is given also as the number of carbon atoms nC on the top-axis of the plot). This plot is compatible with the simplified Simmons equation for tunneling (eq 1). For V = +0.5 V, the linear regression analysis yielded ⟨log|J_0|⟩ = 3.6 ± 0.3 ([J_0] = A·cm^{-2}); this value was statistically indistinguishable from that obtained for V = −0.5 V (⟨log|J_0|⟩ = 3.4 ± 0.3, [J_0] = A·cm^{-2}). These values of J_0 estimate the current density injected across the Ag^{TS}−S and the Ga_2O_3//SAM interfaces into the alkyl chain. For both V = +0.5 and −0.5 V, the slope of the linear regression analysis gave a value of the tunnel decay factor of $\beta = 0.75 \pm 0.02$ Å^{-1} ($\beta = 0.92 \pm 0.02$ nC^{-1}).

The linear decay of the values of log|J| across the full range of lengths suggests that the details of the structure of the SAM—especially liquid-like or crystalline—do *not* influence charge tunneling across these SAMs. Short n-alkanethiolates (n < 5) form SAMs with disordered, liquid-like structures, while long n-

alkanethiolates form compact SAMs with crystalline structure.[52] The fact that the same value of β applies across different lengths of n-alkyl groups, and across different experimental technologies, provides further evidence of a substantial insensitivity of charge transport to the details of the structure of the SAM. In this conclusion, we disagree with recent work by Vilan at al.[58]

Ohmic Electrical Transport through the Ga_2O_3 Layer. The HOPG//Ga_2O_3/EGaIn junction yielded 100% of working junctions. For this junction, J varied linearly with the voltage (Figure 5) and confirmed the ohmic transport across the Ga_2O_3 layer previously reported.[34] Linear regression of the J–V average trace yielded an ohmic conductance (slope) of ~3.0 × 10^3 A·cm^{-2}·V^{-1}, from which we estimated an apparent specific resistance (i.e., the resistance per unit area, and not corrected for the effective electrical contact area) of the Ga_2O_3 layer of $R_{Ga_2O_3}$ = 3.3 × 10^{-4} Ω·cm^2. The measured specific resistance of the Ga_2O_3 layer was lower—by a factor of ~10—than the specific resistance of the SAM of the shortest alkanethiolate SC_1 (R_{SC_1} = 1 × 10^{-3} Ω·cm^2).

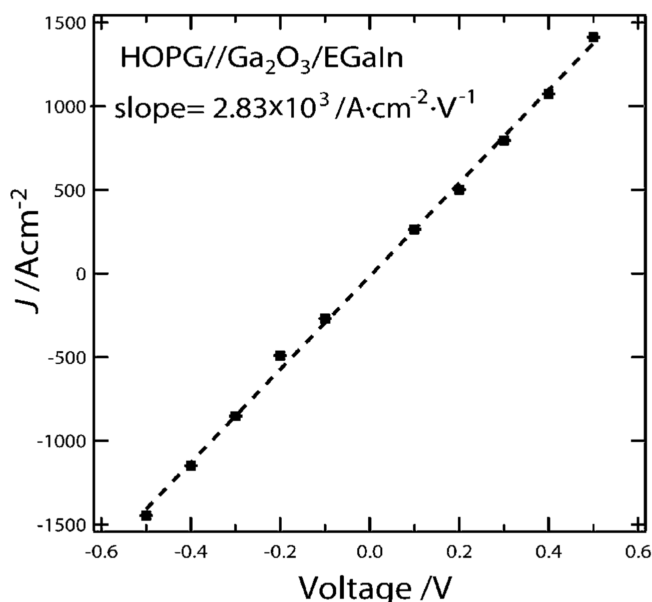

Figure 5. Average J–V curve for HOPG//Ga_2O_3/EGaIn junctions. The slope estimates the specific conductance (conductance per unit area) of the Ga_2O_3 layer of Ga_2O_3/EGaIn conical tips.

In our previous work,[34] we used copper wires with a diameter of 80 μm to estimate a resistance of the Ga_2O_3 layer of $R_{Ga_2O_3}$ = 4 × 10^{-2} Ω·cm^2. We believe that this estimation was less accurate than the new one we report here for two reasons: (i) due to the shape and size of the wires, we were not able to measure accurately the geometrical contact area of the Cu wires on Ga_2O_3/EGaIn droplets, and (ii) we did not take into account the contribution to the resistance of the Cu/CuO_x//Ga_2O_3/EGaIn contact of the native oxide CuO_x passivating the surface of the Cu wires. These Cu/CuO_x//Ga_2O_3/EGaIn contacts, however, exhibited ohmic transport.

The effective electrical contact area of Ag^{TS}-SAM//Ga_2O_3/EGaIn junctions using flattened conical tips was ~10^{-4} the geometrical contact area. To estimate the effective electrical contact area, we calculated the fraction of the surface area available for contact for Ga_2O_3/EGaIn conical tips (α_{tip}), and for Ag^{TS}-SAM substrates (α_{SAM}).

Estimation of α_{tip}. Figure 6 shows the histograms for data for log|J| and the relative Gaussian fits for junctions having structures Fe^{TS}/Fe_2O_3//Hg-drops and Fe^{TS}/Fe_2O_3//Ga_2O_3/EGaIn (flattened conical tips). The resistance of the junction formed with Hg-drops was determined by the specific resistance of the Fe_2O_3 layer. Because, by experimental design, the specific resistance of this Fe_2O_3 layer was ~10^4 the specific resistance of the Ga_2O_3 layer (estimated from measurements of contact resistance of Ga_2O_3/EGaIn tips on HOPG), also the specific resistance of the Ga_2O_3/EGaIn-based junctions was determined by the resistance of the Fe_2O_3 layer. Having approximately the same specific resistance (~$R_{Fe_2O_3}$), at a fixed voltage, both Ga_2O_3/EGaIn conical tips and Hg-drops should have given the same value of current density. The mean value (at V = +0.5 V, ⟨log|J_{tip}|⟩ = −4.2 ± 0.4) of the current density measured with Ga_2O_3/EGaIn conical tips, however, was ~10^{-3} the mean current density measured with the Hg-drop (at V =

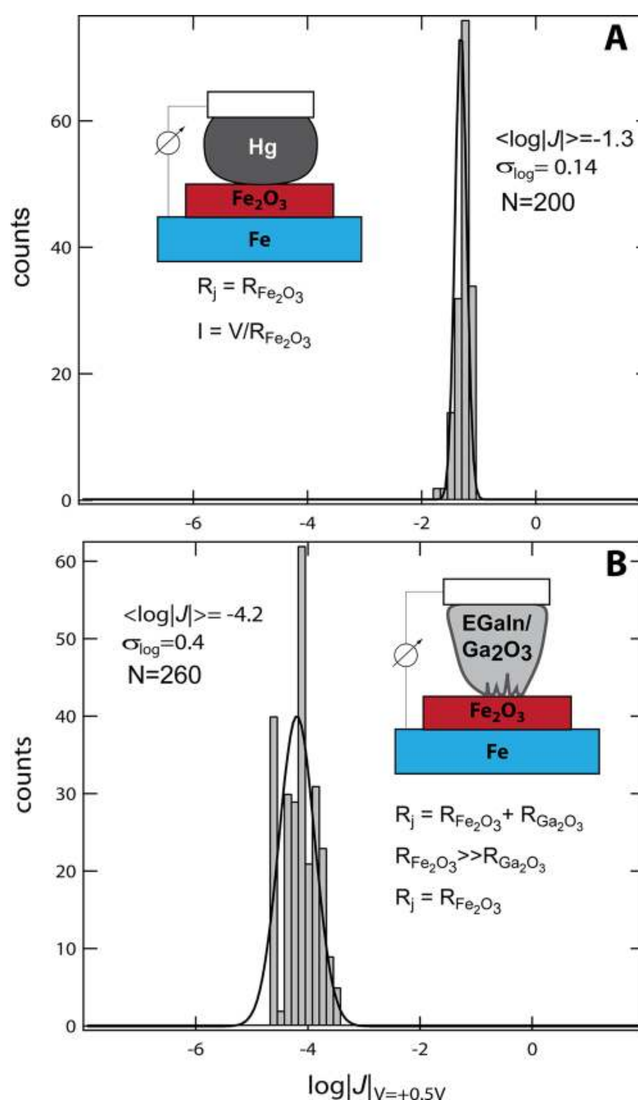

Figure 6. Histograms of the values of log|J| ([J] =A·cm^{-2}) at V = +0.5 V across (A) Fe/Fe_2O_3//Hg junctions and (B) Fe/Fe_2O_3//Ga_2O_3/EGaIn junctions. Solid lines represent Gaussian best fits. We used the same Fe/Fe_2O_3 substrate for all measurements. The resistances (R_J) of junctions A and B were approximately the same ($R_{Fe_2O_3}$) by experimental design.

+0.5 V, $\langle \log|J_{Hg}| \rangle = -1.3 \pm 0.1$). Using these experimental values of current densities, from eq 10 we estimated $\alpha_{tip} = 10^{-3.0\pm0.5}$. We emphasize that, by experimental design, the difference in $J(V)$ between Ga_2O_3/EGaIn and Hg-drop-based junctions cannot be explained by the difference between the resistances of Hg and of the Ga_2O_3 layer.

Estimation of α_{SAM}. Figure 7A shows a STM image of a SAM of SC_{10} on Ag^{TS}. By digital analysis of the pixels (eq 11),

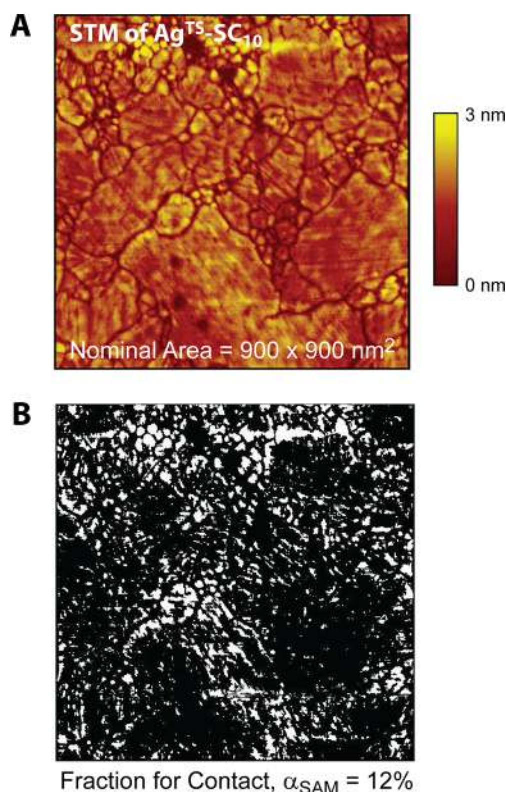

Figure 7. (A) Scanning tunneling microscopy image of a Ag^{TS}-SC_{10} substrate. (B) Surface area available for contact (white area) estimated via digital analysis of the STM image in A. The contact area was estimated as the number of pixels within 2 Å from the top-most average plane of the image. (Lateral profiles of the STM image are reported in Figure S4.)

we estimated that ~12% of the geometrical surface area of the Ag^{TS}-SAM substrate was available for contact (Figure 7B), that is, $\alpha_{SAM} \approx 10^{-1}$. (We reported the STM surface profiles of two different regions of the sample in Figure S4.)

Estimation of the Effective Resistivity of the Ga_2O_3 Layer. Because the surface of HOPG is flat and smooth, for the HOPG//Ga_2O_3/EGaIn junction $A_{elec}/A_{geo} = \alpha_{tip} = 10^{-3}$. We used this value of the ratio A_{elec}/A_{geo} to estimate the value of the effective resistance of the Ga_2O_3 layer as $R_{Ga_2O_3} = 10^{-7}$ Ω·cm^2. This value of $R_{Ga_2O_3}$ leads to a value of the resistivity of the Ga_2O_3 layer of $\rho_{Ga_2O_3} \approx 1$ Ω·cm when we consider an average thickness of this layer of ~1 nm.[41] (The bulk resistivity of EGaIn is $\rho_{Ga_2O_3} = 2.9 \times 10^{-5}$ Ω·cm.[43])

Some aspects of our procedure, however, might lead to an overestimation of $\rho_{Ga_2O_3}$, because the resistance of the HOPG//Ga_2O_3/EGaIn junction might contain contributions from the contact resistance, and because the oxide layer of a conical tip is certainly thicker than 1 nm, at least in some areas. The contact resistance (often called constriction resistance) is a geometrical effect determined by the shapes of microcontacts, and not by their areas[21,24,25,59] (for example, the contact resistance of a circular spot is determined by its radius). A much more accurate estimation of the resistance of the Ga_2O_3 layer than that we provide here would require the estimation of the number, per unit area, of these microcontacts, and the determination of their shapes.

In a previous study[41] we have shown that ~1 nm is the average thickness of the Ga_2O_3 layer on a unstressed droplet of EGaIn. The mechanical manipulation, however, of an EGaIn droplet during the fabrication of a conical tip produces an accumulation of the oxide at the tip apex. It is certain that the thickness of this oxide layer is nonuniform over the whole contact area.

Correction for effective contact area yields $J_0 \approx 10^{7.6\pm0.8}$ A·cm^{-2}. Using, in eq 5, values obtained for the fractions of the surface available for contact respectively for Ga_2O_3/EGaIn conical tips ($\alpha_{tip} = 10^{-3.0\pm0.5}$), and for Ag^{TS}-SAM substrates ($\alpha_{SAM} = 10^{-1}$), for junctions having structure Ag^{TS}-SAM//Ga_2O_3/EGaIn using flattened conical tips, we estimated that the effective electrical contact area is approximately $A_{elec} = 10^{-4.0\pm0.5}A_{geo}$. The correction of the experimental value of $\langle \log|J_0| \rangle$ (Figure 1) for the effective electrical contact area provided an estimate for the injection current density of $\langle \log|J_0| \rangle = 7.6 \pm 0.8$ (J_0/A·cm^{-2}). This corrected value of J_0 was compatible with those estimated for single-molecules approaches,[5−9] and with those reported for large-area junctions using graphene[11] and evaporated-Au[12] top-electrodes used for SAMs formed on flat substrates (Figure 8; we marked as "Ga_2O_3/EGaIn corrected (estimate)" the value of $\langle \log|J_0| \rangle$ corrected for the estimated value of the effective electrical contact area).

■ CONCLUSION

Ga_2O_3/EGaIn-based junctions show a reproducible value of the effective electrical contact area. In this paper, we have described a simple technique for the fabrication of what we call "flattened" Ga_2O_3/EGaIn conical tips. Using these tips reduced the variability in values of $\log|J|$ from $\sigma_{log} = 0.5-1.1$ for as-fabricated tips to $\sigma_{log} \approx 0.3$. The procedure used to flatten the conical tips also retained the convenience of using conical EGaIn top-electrodes.

The comparison of the electrical behavior of smooth Hg-drop top-electrodes with that of flattened (but intrinsically rough) Ga_2O_3/EGaIn conical tips suggests that, in junctions having structure Ag^{TS}-SAM//Ga_2O_3/EGaIn, the effective electrical contact area is $A_{elect} = 10^{-4.0\pm0.5}A_{geo}$, where A_{geo} is the geometrical contact area measured by optical microscopy. This value of A_{elec}—a value that is small, but compatible with estimates of the area of physical contact from measurements of adhesion and friction between surfaces[21−27]—was reproducible from junction to junction. The high reproducibility may perhaps surprise, but it is plausibly attributable to the low compressibility of the SAM, and to the (roughly) constant load applied to the contact. Once a stable contact is formed on top of the SAM (using the observable wrinkling of the tip apex as an intrinsic sensor of the load applied to the junctions), the load applied to the contact cannot be significantly further varied: pushing the Ga_2O_3/EGaIn conical tip against the substrate simply deforms the tip (by making it bulge laterally), and increases (perhaps slightly) the geometrical contact area. We can also infer that following the same procedure for the fabrication of different tips gives surfaces of the Ga_2O_3 layer

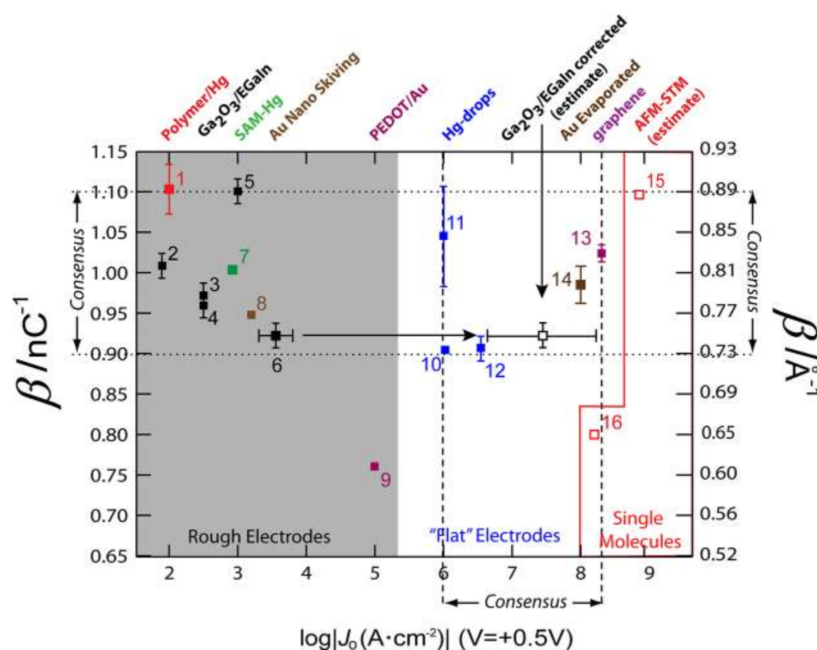

Figure 8. Plot of values of β versus values of $\log|J_0(V = +0.5\ \text{V})|$ reported (filled squares) or estimated (empty squares) for tunneling through n-alkanethiolates with junctions using top-electrodes indicated on the top axis. Numbering is from Table 1. The horizontal arrowed line points to the experimental value of J_0 for Ag^{TS}-SAM//Ga_2O_3/EGaIn corrected for the estimated value of the effective contact area ($A_{elec} = 10^{-4.0\pm0.5}A_{geo}$); the horizontal error bar of this estimate incorporates the uncertainties on the estimation of J_0 from tunneling across SAMs, and on the estimation of the effective electrical contact area. Junctions grouped in the gray zone use either rough top-electrodes or rough bottom-electrodes.

with a reproducible roughness. We believe that the reproducibility of the roughness of the Ga_2O_3 layer and the invariance of the load applied to the SAM//Ga_2O_3/EGaIn contacts result in reproducible values of A_{elec}/A_{geo}.

For Ga_2O_3/EGaIn top-electrodes, the resistance of the oxide layer is not important. For junctions formed with flattened Ga_2O_3/EGaIn conical tips, we observed a linear variation of values of $\langle\log|J|\rangle$ with a constant slope ($\beta = 0.75 \pm 0.02$ Å^{-1}; $\beta = 0.92 \pm 0.02$ nC^{-1}) for tunneling through SAMs of SC_n in the range of lengths from $n = 0$ to $n = 18$. We would not observe this linearity over the complete range (values of current densities varied over 7 orders of magnitude) if the resistance of the Ga_2O_3 layer were contributing to the resistance of the junction.

We do not know, however, if this value of β estimated from measurements of tunneling across Ag^{TS}-SC_n//Ga_2O_3/EGaIn junctions is the true value of β characteristic for tunneling across n-alkanethiolates. Values of β for tunneling through n-alkanethiolates vary by ~20% across different methods (Figure 8); whether this range is due to true variations of the characteristics of SAMs of n-alkanethiolates (e.g., the orientation, order, and density of the packing of the chains, differences in the topography of the supporting metal electrode), or to artifacts characteristic of the different junctions, remains unresolved.

The consensus value of J_0 for tunneling through n-alkanethiolates lies in the range 10^6-10^8 A·cm^{-2} (at V = +0.5 V). For junctions with structure Ag^{TS}-SC_n//Ga_2O_3/EGaIn (conical tips), converting the value of the geometrical contact area (A_{geo}) into the estimated value of the effective electric contact area ($A_{elec} = 10^{-4.0\pm0.5}A_{geo}$) led to a value of the effective injection current density $J_0 = 10^{7.6\pm0.8}$ A·cm^{-2}. This corrected value of J_0 is compatible with those obtained for junctions using smooth and flat electrodes, that is, junctions using electrodes that maximize the value of A_{elec}/A_{geo}. Junctions formed with Hg-drops on top of alkyl chains anchored to silicon surfaces[3,4] yielded $J_0 \approx 10^6-10^{6.5}$ A·cm^{-2}, whereas large-area junctions using flat metal substrates (RMS ≈ 0.7 Å) and flat top-electrodes (e.g., graphene[11]), or conformal, evaporated Au electrodes,[12] yielded rates of charge transport with $J_0 \approx 10^8$ A·cm^{-2}. These results consolidate a consensus value of the injection current for SAMs of n-alkanethiolates in the range 10^6-10^8 A·cm^{-2} (V = +0.5 V) (Figure 8).

Values of $J_0 < 10^6$ A·cm^{-2} (Figure 8, gray field) might imply an overestimation of the effective electrical contact area. In junctions using rough Ga_2O_3/EGaIn top-electrodes, or rough, as-evaporated metal substrates (and using Hg/polymer,[13] or Hg-SAM[15] top-electrodes), the assumption that $A_{elec} = A_{geo}$ leads to values of J_0 in the range 10^2-10^3 A·cm^{-2}. These low experimental values of J_0 cannot be rationalized by a hypothetical high resistance of the top-electrodes: Hg/polymer and Ga_2O_3/EGaIn are highly conductive materials. We believe that, due to the roughness of the electrodes, the value of A_{geo} overestimates the effective electrical area of contact (A_{elec}) of these junctions, thus resulting in an underestimation of J_0.

The value 10^9 A·cm^{-2} might be a hypothetical upper limit to possible experimental estimations of J_0 for SAMs of n-alkanethiolates. We estimated this value of J_0 by extrapolating the value of J_0 (~1×10^{-5} A·mol^{-1}) measured for single n-alkanethiolates in STM-based junctions[5−7,10] (Figure 8) to the value of J_0 for the theoretical number of molecules per cm^2 of the SAM (on Au(111), this number is ~4.5×10^{14} mol·cm^{-2}). This extrapolation assumes that the SAM is free of defects and has a homogeneous density of molecules, and that all the molecules of this ideal SAM are in contact with the top-electrode; these assumptions are unrealistic in experiments with large-area junctions, for which values of J_0 in the range 10^6-10^8 A·cm^{-2} are more probable (Figure 8).

Comparing values of $J_0(V)$ across different methods will require the use of a common standard to take into account

Table 2. Summary of Advantages and Disadvantages of the Most Common Types of Molecular Junctions

top-electrode	advantages	disadvantages
Ga_2O_3/EGaIn	• rapid data collection • high yield (90%) of working junctions • simple design • nondamaging contact • conformal contact • insensitive to contact load • for flattened tips, small dispersion in data for log|J|	• surface roughness • limited range of temperatures • limited range of voltages • subject to adventitious contaminations
Hg-Drops	• well-defined surface • rapid data collection • conformal contact • nondamaging contact • insensitive to contact load	• toxic • volatile • amalgamates with Au and Ag • needs hexadecane bath • surface contamination (high surface energy)
Hg-SAM	• rapid data collection • conformal contact • nondamaging contact • insensitive to contact load	• toxic • amalgamates with Au and Ag • needs hexadecane bath • intercalation of molecules from the top-SAM into the bottom-SAM might occur • possible lateral movement, or exchange of SAM on Hg
Graphene	• well-defined top-interface • high stability • high durability • high yield • resistant to a broad range of temperatures • usable at high voltages	• complicated experimental protocol • sensitive to load applied to contact • time consuming
Single Molecules (STM, AFM)	• rapid collection of data • resistant to a broad range of temperatures • usable at high voltages	• unknown number of contacted molecules • complicated experimental protocol • time consuming • high equipment cost • sensitive to contact load
Conductive Polymers	• durability	• requires thermal annealing that can damage the SAM • complicated design • possible intercalation of molecules into the SAM • sensitive to load • time consuming
Evaporated Au	• conformal contact	• damaging contact • formation of filaments • difficult experimental protocol • time consuming

differences in measured values of $J(V)$. The values of A_{elec}/A_{geo} for these different techniques are unknown; in addition, a number of factors other than the value of the ratio A_{elec}/A_{geo} might contribute to the variability of the values of J_0 within the consensus range; these parameters include the nature of the top- and bottom-contacts (e.g, covalent or van der Waals), the nature of the materials used as electrodes, and the presence of contaminants. We recommend using SAMs of SC_{10} and SC_{16} as standards for the calibration of values of $J(V)$.

The value of the effective electrical contact area is not important in physical-organic studies; its reproducibility is important. Using Ga_2O_3/EGaIn flattened conical tips as top-electrodes yielded a (roughly) constant value of the standard deviation ($\sigma_{log} \approx 0.3$) of the value of log|J| across SAMs of individual *n*-alkanethiolates, and a value of the tunneling decay factor $\beta = 0.75 \pm 0.02$ Å^{-1} (or $\beta = 0.92 \pm 0.02$ nC^{-1}) that falls in the 90% consensus range of values of β estimated by different techniques (Figure 8). These results indicate that, in Ag^{TS}-SAM//Ga_2O_3/EGaIn junctions, the value of A_{elec}/A_{geo} is (surprisingly) reproducible from junction to junction, and that variations of measured values of tunneling currents across different SAMs are primarily due to differences in the lengths of the *n*-alkanethiolates. The dispersion in data collected with flattened Ga_2O_3/EGaIn conical tips was smaller than that observed for as-fabricated conical tips; flattening of the tips, however, had no effect on the mean values (i.e., ⟨log |J|⟩) of the distributions of experimental values of log|J|.

Ga_2O_3/EGaIn top-electrodes are a convenient methodology for physical-organic studies of charge tunneling. Table 2 summarizes advantages and disadvantages that we identified for the most common techniques used for studying charge transport through molecules anchored to conductive

substrates. From this comparison, Ga_2O_3/EGaIn top-electrodes emerge as a particularly convenient technology for physical-organic studies of charge transport through molecules. Physical-organic approaches, which examine only trends in $J(V)$ as a function of the structure of the molecules making up the SAM, require that the properties of the top- and bottom-interfaces of these different types of junction are unchanged across a series of measurements. The roughness of the Ga_2O_3 layer gives an uncertain morphology to the SAM//Ga_2O_3 interface, but, so long as the properties of this interface remain constant, physical-organic protocols can be applied to the study of charge transport through SAMs, even though the SAM//Ga_2O_3 interface is not well defined. (None of the interfaces of the methods listed in Table 2 is, however, entirely defined.)

The simplicity and rapidity in assembling junctions using Ga_2O_3/EGaIn top-electrodes that make it possible to collect large numbers of data ($\sim 10^3$ per day) are currently unmatched by any other method listed in Table 2. We stress that collection of large numbers of data is critical to validating the statistical significance of studies of structure−tunneling relationships by physical-organic protocols.

Ga_2O_3/EGaIn tips do not damage the SAM. Ga_2O_3/EGaIn top-electrodes enable a rapid collection of data because they do not require a fine control of the load to form nondamaging contacts on top of the SAM. The load applied to contacts using soft Ga_2O_3/EGaIn conical tips—or liquid metal electrodes in general—cannot be significantly varied; pushing the Ga_2O_3/EGaIn electrode against the sample simply increases the geometrical contact area of the junction. By contrast, small variations of the load applied to junctions using solid top-electrodes might change the effective electrical contact area, deform the SAM, and even damage the SAM. With only the exception of Hg-based junctions, all other methods listed in Table 2 use solid top-electrodes; the loads applied to these contacts, however, have never been reported.

Ga_2O_3/EGaIn is an affordable technology that might allow comparison of results obtained in different laboratories. Several years of work in our laboratory have proved that EGaIn-based junctions are a practical and convenient methodology for physical-organic studies of charge tunneling through SAMs.

So far, the effect of the resistance of the Ga_2O_3 layer on the electrical behavior of the junctions, and the value of the effective electrical contact area between SAMs and Ga_2O_3/EGaIn conical tips, have been two major unresolved issues in the interpretation of data obtained with EGaIn-based junctions. In this paper we have shown that the resistance of the Ga_2O_3 layer is not important, and that the effective electrical contact area—which is $\sim 10^{-4}$ the geometrical contact area—is reproducible across different experiments; the correction of current densities for this value of the effective electrical contact area led to results for tunneling across *n*-alkanethiolates compatible with those reported for techniques far more complex and expensive than Ga_2O_3/EGaIn electrodes.

Using Ga_2O_3/EGaIn top-electrodes still requires attention to experimental details (especially the fabrication of the conical tips), but the procedure needs only a few days to learn. The simple (and inexpensive) fabrication of EGaIn-based junctions can be replicated in any laboratory, and the availability of very well-defined reference data (such those of Figure 1) for comparison, calibration, and use as standards makes comparisons among data generated in different laboratories straightforward.

■ ASSOCIATED CONTENT

Supporting Information

Experimental details, including a video showing the procedure for the fabrication of flattened Ga_2O_3/EGaIn conical tips. This material is available free of charge via the Internet at http://pubs.acs.org.

■ AUTHOR INFORMATION

Corresponding Author

gwhitesides@gmwgroup.harvard.edu

Notes

The authors declare no competing financial interest.

■ ACKNOWLEDGMENTS

This work was supported by a subcontract from Northwestern University from the Department of Energy (DE-SC0000989) for work on synthesis of materials and measurements of charge transport.

■ REFERENCES

(1) Simmons, J. G. *J. Appl. Phys.* **1963**, *34*, 1793.
(2) Simmons, J. G. *J. Appl. Phys.* **1963**, *34*, 2581.
(3) Vilan, A.; Yaffe, O.; Biller, A.; Salomon, A.; Kahn, A.; Cahen, D. *Adv. Mater.* **2010**, *22*, 140.
(4) Yaffe, O.; Scheres, L.; Segev, L.; Biller, A.; Ron, I.; Salomon, A.; Giesbers, M.; Kahn, A.; Kronik, L.; Zuilhof, H.; Vilan, A.; Cahen, D. *J. Phys. Chem. C* **2010**, *114*, 10270.
(5) Xu, B. Q.; Tao, N. J. J. *Science* **2003**, *301*, 1221.
(6) Chen, F.; Li, X. L.; Hihath, J.; Huang, Z. F.; Tao, N. J. *J. Am. Chem. Soc.* **2006**, *128*, 15874.
(7) Suzuki, M.; Fujii, S.; Fujihira, M. *Jpn. J. Appl. Phys., Part 1* **2006**, *45*, 2041.
(8) Engelkes, V. B.; Beebe, J. M.; Frisbie, C. D. *J. Am. Chem. Soc.* **2004**, *126*, 14287.
(9) Beebe, J. M.; Engelkes, V. B.; Miller, L. L.; Frisbie, C. D. *J. Am. Chem. Soc.* **2002**, *124*, 11268.
(10) Wierzbinski, E.; Yin, X.; Werling, K.; Waldeck, D. H. *J. Phys. Chem. B* **2012**, *117*, 4431.
(11) Wang, G.; Kim, Y.; Choe, M.; Kim, T. W.; Lee, T. *Adv. Mater.* **2011**, *23*, 755.
(12) Kim, T. W.; Wang, G. N.; Lee, H.; Lee, T. *Nanotechnology* **2007**, 18.
(13) Milani, F.; Grave, C.; Ferri, V.; Samori, P.; Rampi, M. A. *ChemPhysChem* **2007**, *8*, 515.
(14) Weiss, E. A.; Chiechi, R. C.; Kaufman, G. K.; Kriebel, J. K.; Li, Z. F.; Duati, M.; Rampi, M. A.; Whitesides, G. M. *J. Am. Chem. Soc.* **2007**, *129*, 4336.
(15) Holmlin, R. E.; Haag, R.; Chabinyc, M. L.; Ismagilov, R. F.; Cohen, A. E.; Terfort, A.; Rampi, M. A.; Whitesides, G. M. *J. Am. Chem. Soc.* **2001**, *123*, 5075.
(16) Simeone, F. C.; Rampi, M. A. *Chimia* **2010**, *64*, 362.
(17) Nijhuis, C. A.; Reus, W. F.; Barber, J. R.; Dickey, M. D.; Whitesides, G. M. *Nano Lett.* **2010**, *10*, 3611.
(18) Reus, W. F.; Nijhuis, C. A.; Barber, J. R.; Thuo, M. M.; Tricard, S.; Whitesides, G. M. *J. Phys. Chem. C* **2012**, *116*, 6714.
(19) Thuo, M. M.; Reus, W. F.; Nijhuis, C. A.; Barber, J. R.; Kim, C.; Schulz, M. D.; Whitesides, G. M. *J. Am. Chem. Soc.* **2011**, *133*, 2962.
(20) Nijhuis, C. A.; Reus, W. F.; Barber, J. R.; Whitesides, G. M. *J. Phys. Chem. C* **2012**, *116*, 14139.
(21) Holm, R. *Electric Contacts: Theory and Applications*; Springer: Berlin, 2001.
(22) Greenwood, J. A.; Williamson, J. B. P. *Proc. R. Soc. London, Ser. A* **1966**, 295.
(23) Tabor, D. *J. Colloid Interface Sci.* **1977**, *58*, 2.
(24) Slate, P. G. *Electrical Contacts: Principles and Applications*; Marcel Dekker, Inc.: New York, 1999.

(25) Bowder, F. P.; Tabor, D. *The Friction and Lubrication of Solids*; Oxford University Press: Oxford, 2001.
(26) Adamson, A. W. *Physical Chemistry of Surfaces*; John Wiley & Sons, Inc.: New York, 1997.
(27) Demirel, A. L.; Granick, S. *J. Chem. Phys.* **1998**, *109*, 6889.
(28) Metzger, R. M.; Baldwin, J. W.; Shumate, W. J.; Peterson, I. R.; Mani, P.; Mankey, G. J.; Morris, T.; Szulczewski, G.; Bosi, S.; Prato, M.; Comito, A.; Rubin, Y. *J. Phys. Chem. B* **2003**, *107*, 1021.
(29) Stewart, D. R.; Ohlberg, D. A. A.; Beck, P. A.; Chen, Y.; Williams, R. S. *Nano Lett.* **2004**, *4*, 133.
(30) Lau, C. N.; Stewart, D. R.; Williams, R. S.; Bockrath, M. *Nano Lett.* **2004**, *4*, 569.
(31) Akkerman, H. B.; de Boer, B. *J. Phys.: Condens. Matter* **2008**, *20*, 013001.
(32) Salomon, A.; Cahen, D.; Lindsay, S.; Tomfohr, J.; Engelkes, V. B.; Frisbie, C. D. *Adv. Mater.* **2003**, *15*, 1881.
(33) Nijhuis, C. A.; Reus, W. F.; Siegel, A. C.; Whitesides, G. M. *J. Am. Chem. Soc.* **2011**, *133*, 15397.
(34) Nijhuis, C. A.; Reus, W. F.; Whitesides, G. M. *J. Am. Chem. Soc.* **2009**, *131*, 17814.
(35) Nijhuis, C. A.; Reus, W. F.; Whitesides, G. M. *J. Am. Chem. Soc.* **2010**, *132*, 18386.
(36) Thuo, M. M.; Reus, W. F.; Simeone, F. C.; Kim, C.; Schulz, M. D.; Yoon, H. J.; Whitesides, G. M. *J. Am. Chem. Soc.* **2012**, *134*, 10876.
(37) Yoon, H. J.; Shapiro, N. D.; Park, K. M.; Thuo, M. M.; Soh, S.; Whitesides, G. M. *Angew. Chem., Int. Ed.* **2012**, *51*, 4658.
(38) Fracasso, D.; Valkenier, H.; Hummelen, J. C.; Solomon, G. C.; Chiechi, R. C. *J. Am. Chem. Soc.* **2011**, *133*, 9556.
(39) Nerngchamnong, N.; Yuan, L.; Qi, D.-C.; Li, J.; Thompson, D.; Nijhuis, C. A. *Nat. Nanotechnol.* **2013**, *8*, 113.
(40) Fracasso, D.; Mugladi, M. I.; Rohwerder, M.; Terfort, A.; Chiechi, R. C. *J. Phys. Chem. C* **2013**, *117*, 11367.
(41) Cademartiri, L.; Thuo, M. M.; Nijhuis, C. A.; Reus, W. F.; Tricard, S.; Barber, J. R.; Sodhi, R. N. S.; Brodersen, P.; Kim, C.; Chiechi, R. C.; Whitesides, G. M. *J. Phys. Chem. C* **2012**, *116*, 10848.
(42) Reus, W. F.; Thuo, M. M.; Shapiro, N. D.; Nijhuis, C. A.; Whitesides, G. M. *ACS Nano* **2012**, *6*, 4806.
(43) Dickey, M. D.; Chiechi, R. C.; Larsen, R. J.; Weiss, E. A.; Weitz, D. A.; Whitesides, G. M. *Adv. Funct. Mater.* **2008**, *18*, 1097.
(44) Chiechi, R. C.; Weiss, E. A.; Dickey, M. D.; Whitesides, G. M. *Angew. Chem., Int. Ed.* **2008**, *47*, 142.
(45) McCreery, R. L.; Yan, H.; Bergren, A. J. *Phys. Chem. Chem. Phys.* **2013**, *15*, 1065.
(46) Weiss, E. A.; Kaufman, G. K.; Kriebel, J. K.; Li, Z. F.; Schalek, R.; Whitesides, G. M. *Langmuir* **2007**, *23*, 9686.
(47) Akkerman, H. B.; Naber, R. C. G.; Jongbloed, B.; van Hal, P. A.; Blom, P. W. M.; de Leeuw, D. M.; de Boer, B. *Proc. Natl. Acad. Sci. U.S.A.* **2007**, *104*, 11161.
(48) Salomon, A.; Boecking, T.; Seitz, O.; Markus, T.; Amy, F.; Chan, C.; Zhao, W.; Cahen, D.; Kahn, A. *Adv. Mater.* **2007**, *19*, 445.
(49) York, R. L.; Nguyen, P. T.; Slowinski, K. *J. Am. Chem. Soc.* **2003**, *125*, 5948.
(50) Slowinski, K.; Fong, H. K. Y.; Majda, M. *J. Am. Chem. Soc.* **1999**, *121*, 7257.
(51) Pourhossein, P.; Chiechi, R. C. *ACS Nano* **2012**, *6*, 5566.
(52) Love, J. C.; Estroff, L. A.; Kriebel, J. K.; Nuzzo, R. G.; Whitesides, G. M. *Chem. Rev.* **2005**, *105*, 1103.
(53) Liao, K. C.; Simeone, F. C.; Whitesides, G. M., unpublished observations.
(54) Huisman, E. H.; Guedon, C. M.; van Wees, B. J.; van der Molen, S. J. *Nano Lett.* **2009**, *9*, 3909.
(55) Haag, R.; Rampi, M. A.; Holmlin, R. E.; Whitesides, G. M. *J. Am. Chem. Soc.* **1999**, *121*, 7895.
(56) Slowinski, K.; Majda, M. *J. Electroanal. Chem.* **2000**, *491*, 139.
(57) Beebe, J. M.; Kim, B.; Frisbie, C. D.; Kushmerick, J. G. *ACS Nano* **2008**, *2*, 827.
(58) Levine, I.; Weber, S. M.; Feldman, Y.; Bendikov, T.; Cohen, H.; Cahen, D.; Vilan, A. *Langmuir* **2012**, *28*, 404.
(59) Greenwood, J. A. *Br. J. Appl. Phys.* **1966**, *17*, 1621.